Origin of the imbalance between energy cascade and dissipation in turbulence

P. C. Valente,[1,*] R. Onishi,[2] and C. B. da Silva[1]

[1]*LAETA/IDMEC, Instituto Superior Técnico, Universidade de Lisboa, Av. Rovisco Pais, 1049-001 Lisboa, Portugal*

[2]*Center for Earth Information Science and Technology, JAMSTEC, 3173-25 Showa-machi, Kanazawa-ku, Yokohama, Kanagawa 236-0001, Japan*

(Received 27 February 2014; published 8 August 2014)

It is shown in direct numerical simulations of homogeneous isotropic non-stationary turbulence that there is a systematic and significant imbalance between the non-linear energy cascade to fine scales and its dissipation. This imbalance stems from the power required to induce or annihilate fine-scale motions in order to change the level of dissipation. The imbalance is present regardless of transfer time-lags and is applicable to a wide range of Reynolds numbers.

DOI: 10.1103/PhysRevE.90.023003 PACS number(s): 47.27.W−, 47.27.E−

Turbulence is nature's way of speeding up molecular transport in fluids and plasmas by generating multiscale random motions, and is crucial for a diverse range of phenomena, including rain initiation [1], the formation of planets [2], and predator-prey or mating interactions [3]. It is widely accepted that the induced motions are fed by a continuous range of larger-scale motions—the energy cascade [4]—and are always sufficiently fine-scale to make molecular transport efficient—sometimes referred to as dissipation anomaly [4,5]. An essential ingredient underlying turbulence models and theories is that these fine-scale turbulent motions are very fast-paced and thus instantaneously adjust to dissipate whatever energy they are fed. This concept became popularised as Kolmogorov's four-fifth's law in its isotropic form [4,6].

However, this near-instantaneous adjustment between the cascade flux Π and the dissipation ε, which is trivial for stationary flows, is yet to be observed in non-stationary turbulent flows [7]. One viewpoint is that for non-stationary flows the balance $\Pi \approx \varepsilon$ is only valid for very large Taylor microscale Reynolds numbers, $\mathrm{Re}_\lambda = \mathcal{O}(10^5)$, which turns out to be one order of magnitude larger than the Reynolds numbers characteristic of turbulence in the atmosphere, $\mathrm{Re}_\lambda = \mathcal{O}(10^{3-4})$ [8]. This range of Reynolds numbers is far beyond what is presently achievable in either simulations or experiments of non-stationary turbulence [$\mathrm{Re}_\lambda = \mathcal{O}(10^3)$], and therefore these have failed to provide more than a few data points supporting this belief [9]. An alternative viewpoint is that there is a time-lag in the energy transfer mechanism as the energy is cascaded through the inertial-range down to the finest scales and therefore $\Pi \neq \varepsilon$ for non-stationary flows [10].

We report further evidence of an instantaneous global imbalance between Π and ε in direct numerical simulations (DNS) of non-stationary homogeneous turbulence with (i) a time varying external power input [10,11] and (ii) freely decaying in the absence of external forcing. We show that in these flows the non-linear flux Π follows closely the temporal variations of the kinetic energy K and integral length-scale ℓ with virtually no delay, i.e., $\Pi \sim K^{3/2}/\ell$, whereas the dissipation strongly departs from this classical scaling, similar to what has been observed in recent experiments [12,13].

Based on our DNS data, we propose that there is a basic underlying mechanism driving the imbalance between Π and ε, which is present regardless of energy transfer time-lags. Specifically, our data indicate that the power required to change the kinetic energy of the fine scales (and thus the level of dissipation) is non-negligible and is supplied by the difference between the power injected into the dissipative scales, i.e., Π, and the power dissipated, ε. Therefore, our data, together with the experimental evidence of non-negligible imbalances between Π and ε in decaying flows up to $\mathrm{Re}_\lambda = \mathcal{O}(10^4)$ [9], conspires to the conclusion that at least for Reynolds numbers of practical use for engineering and geophysics it is not possible to change the level of dissipation without having a transient imbalance between Π and ε. With this mechanism we are also able to explain discrepancies between the numerical values of the normalised energy dissipation rates in stationary and non-stationary turbulent flows [14], and support the examples of non-equilibrium dissipative behavior observed in recent experiments [12,13].

Our data are obtained by integrating the Navier-Stokes equations in a periodic box of size 2π with a standard pseudo-spectral scheme, de-aliased with the 2/3 rule, and a third-order Runge-Kutta in time [15]. A transient state is induced by a time-varying power input $P(t)$ supplied by an external isotropic forcing $f(k,t)$ δ-correlated in time [16] following a square-wave protocol [11] (see Fig. 1). An additional simulation is performed where the forcing is switched off to mimic freely decaying turbulence (see Fig. 2). For the square-wave power input cases, the external force injects energy within the first four wave numbers so that the integral-scale $\ell(t)$ [$\ell(t) \equiv \pi/(2K(t)) \int_0^\infty E(k,t)/k\,dk$, where $K(t) \equiv \int_0^\infty E(k,t)\,dk$ is the turbulent kinetic energy and $E(k,t)$ the power spectrum of velocity fluctuations] is at least 9 times smaller than the size of the periodic box throughout the simulation. For the statistically steady simulation used as an initial condition for the freely decaying DNS the first five wave numbers are forced such that ℓ is 1/15 of the box size to avoid confinement effects [17] (see Table I). The statistics are obtained by averaging over the whole domain for a given snapshot which provides c.a. 1000 uncorrelated samples (based on the ratio between the box size and the integral scale) and allows to track statistical quantities in time. Prior to introducing the square-wave varying power input

*pedro.cardoso.valente@ist.utl.pt

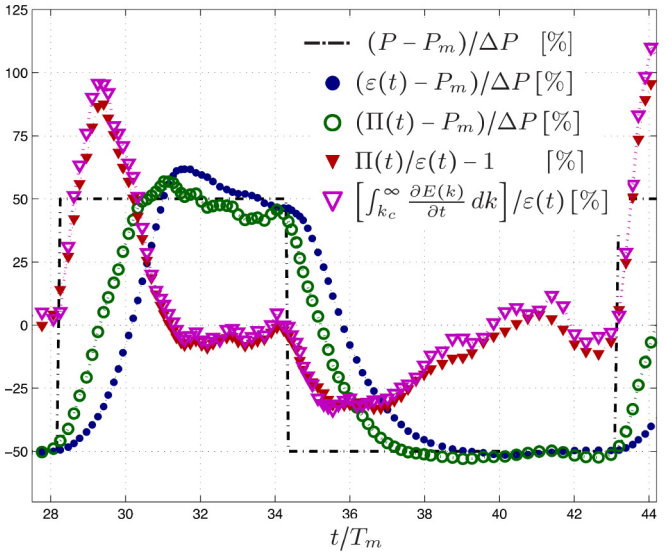

FIG. 1. (Color online) The imbalance between Π and ε in a DNS of non-stationary turbulence with varying power input $P(t)$ (dataset 1). The difference between the two energy fluxes, $\Pi-\varepsilon$, increases/decreases the kinetic energy of the fine scales at the rate $\int_{k_c}^{\infty}\partial E(k)/\partial t\,dk$ [see Eq. (2)]. Π, ε and P are normalized with the mean and amplitude of the square-wave power input cycle (P_m and ΔP) so that they vary around $\pm 50\%$. The abscissa is normalised by the average turnover time T_m.

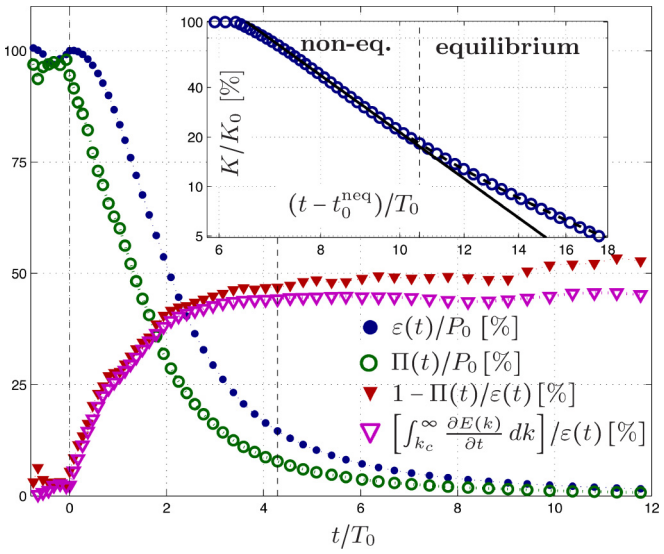

FIG. 2. (Color online) The increasing imbalance between Π and ε in a DNS of freely decaying turbulence and the corresponding increasing kinetic energy loss rate of the fine scales, $\int_{k_c}^{\infty}\partial E(k)/\partial t\,dk$ [see Eq. (2)]. For $t/T_0 \gtrapprox 4$ an equilibrium period is reached where $\Pi/\varepsilon \approx 1/2$. The small, but increasing difference between $\Pi-\varepsilon$ and $\int_{k_c}^{\infty}\partial E(k)/\partial t\,dk$ is due to differences between ε and ε' as the Reynolds number decreases. In the inset, the decay of kinetic energy K is fitted with a power-law $K/K_0 \sim (t+t_0)^{-n}$ yielding $n=3.5$ and $n=1.4$ for the non-equilibrium and equilibrium periods, respectively. The data (excluding the first five data points) are fitted with the non-linear method discussed in Ref. [18]. P_0, K_0, and $T_0=\ell_0/\sqrt{K_0}$ are the initial power input, kinetic energy, and turnover time, respectively, and $t_0^{\rm neq}$ is the virtual time origin for the non-equilibrium power-law fit.

TABLE I. Overview of our DNSs with square-wave power input (datasets 1 and 2) and freely decaying (dataset 3). Note that N and $\eta\equiv(\nu^3/\varepsilon)^{1/4}$ are, respectively, the number of colocation points and the Kolmogorov length-scale. Re_0 is a reference Reynolds number defined in the caption of Fig. 3.

#	N	$P\vert_{\rm min}^{\rm max}$	ν	$\mathrm{Re}_0\vert_{\rm min}^{\rm max}$	$\mathrm{Re}_\lambda\vert_{\rm min}^{\rm max}$	$(2\pi/\ell)\vert_{\rm min}^{\rm max}$	$(k\eta)\vert_{\rm min}^{\rm max}$
1	512	30/6	0.008	107/82	147/72	11/9	3.0/1.9
2	1024	30/6	0.0027	191/146	261/138	11/9	2.6/1.7
3	512	96/0	0.008	115/-	115/45	15/10	3.5/1.4

(or switching off the forcing) the simulation is allowed to run for several turnover times, $\ell/\sqrt{K}$, until a statistical steady state is ensured and the turbulence is fully developed.

The strong imbalance between Π and ε in both non-stationary situations can be appreciated in Figs. 1 and 2 where our data indicates that Π/ε can be as large as 2 and as small as 0.5 (with and without forcing, respectively) and appears as a 'delay' between Π and ε when the two quantities are plotted in time. It is worth noting that the imbalance observed here is obtained in strong turbulence characterised by moderately large Reynolds numbers, up to $\mathrm{Re}_\lambda=260$, where $\mathrm{Re}_\lambda\equiv\sqrt{2K/3}\,\lambda/\nu$ and $\lambda\equiv\sqrt{10\nu K/\varepsilon}$ is the Taylor microscale (see Table I).

To show the origin of this imbalance we use the power balance equation in wave number space for homogeneous turbulence [4],

$$\frac{\partial E(k,t)}{\partial t}=T(k,t)-2\nu k^2E(k,t)+f(k,t), \qquad (1)$$

where E, $2\nu k^2E$, T, and f are, respectively, the spectra of kinetic energy of velocity fluctuations, energy dissipation, energy transfer, and power input (which integrate to K, ε, 0, and P) and k and ν are the wave number and the kinematic viscosity of the fluid, respectively. For homogeneous turbulence with a prescribed power input, the transfer spectrum $T(k,t)$ has a single zero crossing (at $k=k_c$) as long as $\nu\neq 0$ (see [19] and Appendix A). This single zero crossing is the location of the maximum non-linear energy flux $\Pi\equiv-\int_0^{k_c}T(k,t)\,dk=\int_{k_c}^{\infty}T(k,t)\,dk$ and therefore it is convenient to use k_c as a reference to distinguish between the wave numbers $k<k_c$ which on net loose kinetic energy via non-linear interactions, from the wave numbers $k\geqslant k_c$ which on net receive it. The wave numbers $k\geqslant k_c$ include the inertial range, which according to Kolmogorov's phenomenology would lead to a dissipation spectrum following $2\nu k^2E(k,t)\sim\nu\varepsilon^{2/3}k^{1/3}$ prior to rolling off exponentially in the deep dissipative range [4]. Therefore it follows that the inertial range has a non-negligible contribution to the overall dissipation, even at very high Reynolds numbers as can be readily confirmed by a model spectrum (see Appendix A). We therefore denote the wave numbers $k<k_c$ as large-scales and the wave numbers $k\geqslant k_c$ as dissipative scales. Naturally, the choice of the cutoff to separate between large and dissipative scales is not unique. Nevertheless, our particular choice makes the following analyses precise and allows to directly relate quantities to the maximum energy transfer.

By integrating Eq. (1) within $k_c \leqslant k < \infty$ it follows that the power being fed into the kinetic energy of dissipative scales [$\equiv \int_{k_c}^{\infty} \partial E(k,t)/\partial t\, dk$] is exactly the difference between the maximum energy cascade flux Π and the dissipation within these scales $\varepsilon'(\equiv 2\nu \int_{k_c}^{\infty} k^2 E(k,t)\, dk)$, i.e.,

$$\int_{k_c}^{\infty} \frac{\partial E(k,t)}{\partial t}\, dk = \Pi(t) - \varepsilon'(t). \tag{2}$$

Note that for the Reynolds number of our simulations the dissipation within large scales ($k < k_c$) is negligible and thus $\varepsilon' \approx \varepsilon$ (although less so in the freely decay simulation for large times due to low Re_λ, see Fig. 2). Furthermore, because we treat the dissipative scales (including those within the inertial range) as a whole, any cascade transfer lag delaying the arrival of the maximum energy flux Π at k_c to any given wave number $k > k_c$ is averaged out, isolating the fact that imbalances between Π and ε' are only linked to changes in the kinetic energy of the dissipative scales, viz. Eq. (2). In other words, since $\Pi \equiv \int_{k_c}^{\infty} T(k,t)\, dk$, the actual shape of the transfer spectrum $T(k,t)$ as well as cascade time-lag effects do not come into play. This demonstrates the inability of the cascade time-lag hypothesis in explaining the imbalance between Π and ε observed in our data (Figs. 1 and 2).

In contrast, our data strongly suggest that imbalances between Π and ε' are the root cause for the changes in the level of dissipation. To see this, notice that changes in the level of dissipation require changes in the kinetic energy of the dissipative scales [since their spectra are proportional, cf. Eq. (1)] and that the power required to change their kinetic energy can only be supplied by $\Pi - \varepsilon'$ as shown by Eq. (2). This can also be seen within Kolmogorov's phenomenology [4] by noticing that changes in the level of dissipation ($\Delta\varepsilon$) require changes in the kinetic energy of fine scales (ΔK_η) and thus demand a non-negligible power of the order of $\Delta K_\eta/\tau_\eta \sim \Delta\varepsilon$ (where $K_\eta \sim \sqrt{\varepsilon\nu}$ and $\tau_\eta \sim \sqrt{\nu/\varepsilon}$ are Kolmogorov's estimates for fine-scale kinetic energy and time-scale; note that $\Delta K_\eta = \partial K_\eta/\partial\varepsilon\, \Delta\varepsilon \sim \sqrt{\nu/\varepsilon}\, \Delta\varepsilon$).

It can also be shown that imbalances between Π and ε' are directly caused by the rate of change of Π, and not by the rate of change of ε as previously thought [10]. This can be shown by expanding $T(k,t)$ and $E(k,t)$ with a Taylor series around t_0, corresponding to an instant where the forcing is switched off, and introducing it in Eq. (1) to conclude that to a leading order,

$$\Pi(t) - \varepsilon'(t) = (\partial\Pi(t)/\partial t)_{t=t_0} t + \mathcal{O}(t^2), \tag{3}$$

(see Appendix B for the derivation).

Owing to the dissipation anomaly it is customary to consider an inviscid estimate of the level of dissipation and energy cascade flux based solely on large scale turbulence quantities. In particular, it is commonly assumed that the dissipation ε is proportional to the kinetic energy K over a large-scale eddy turnover time $\ell/\sqrt{K}$, i.e., $\varepsilon \propto C_\varepsilon K^{3/2}/\ell$, where C_ε is a constant [4,10]. The same inviscid estimate applies to Π, i.e., $C_\Pi \propto \Pi\ell/K^{3/2} \approx$ constant [20]. We test these two scalings separately and observe that the scaling $C_\Pi \approx$ constant is a good approximation, even when the imbalance between Π and ε is large (see Fig. 3 and note that $C_\Pi = 0.55 \pm 0.07$ covers both free decay and the transients induced by the power input cycles). On the other hand, the classical scaling $C_\varepsilon \approx$ constant breaks down during the transients induced by the power input cycles. Instead C_ε varies substantially with the local Reynolds number, approximately following a power-law (see Fig. 3). This strongly indicates that the non-linear energy flux Π follows closely the evolution of the large-scale quantities (K and ℓ) whereas ε does not, due to the imbalance between the two. A similar behavior was recently demonstrated experimentally in non-equilibrium regions of grid-generated decaying turbulence [12,13]. Indeed, our freely decaying data allow to qualitatively recover three main results of these recent wind-tunnel experiments, namely, (i) the existence of a non-equilibrium region with $C_\varepsilon \sim \mathrm{Re}_\lambda^{-\alpha}$ [12] prior to the classical equilibrium state where $C_\varepsilon \approx$ constant (see Fig. 3 and Refs. [12,14,21]), (ii) the different regions lead to kinetic energy decay power-laws, $K \sim (t + t_0)^{-n}$, with a significantly larger exponent during the non-equilibrium (see Figs. 2 and Ref. [18]) and (iii) $C_\Pi \approx$ constant is a good approximation throughout both regions of the decay (see Fig. 3 and Ref. [13]).

Note that the values spanned by our DNSs, $45 \leqslant \mathrm{Re}_\lambda \leqslant 260$, are comparable with the wind-tunnel experiments [12,13]. Also note that we define the statistical quantities so that they can be directly compared with the experimentally measured surrogates.

Furthermore our data hint to a different interpretation of the equilibrium behavior (i.e., $C_\varepsilon \approx$ constant) observed in freely decaying turbulence for large times after the start of the decay (e.g., far downstream from the turbulence generating grids in a wind tunnel). The increasing difference between Π and ε observed throughout the non-equilibrium (c.f. Fig. 2) implies that the fine-scale kinetic energy loss-rate [i.e., $\int_{k_c}^{\infty} \partial E(k,t)/\partial t\, dk$] is an increasing fraction of the dissipation. Our data further suggests that a new equilibrium is reached

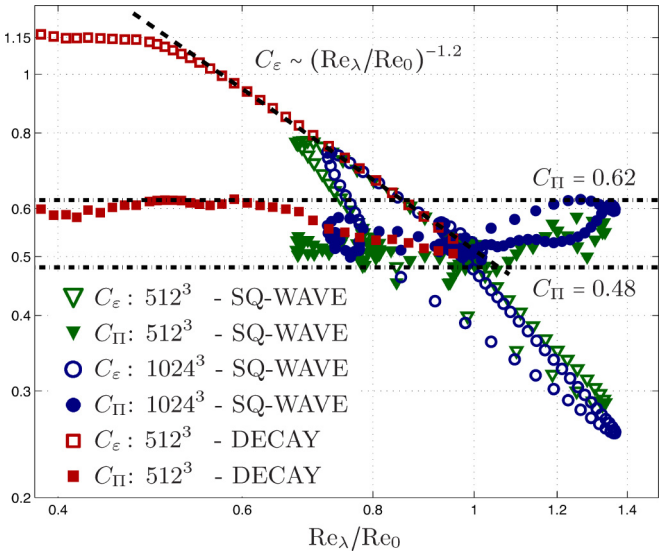

FIG. 3. (Color online) Normalized energy dissipation $C_\varepsilon \equiv (3/2)^{5/2}\varepsilon\, \ell/K^{3/2}$ and energy cascade flux $C_\Pi \equiv (3/2)^{5/2}\Pi\, \ell/K^{3/2}$ versus normalized local Reynolds number $\mathrm{Re}_\lambda/\mathrm{Re}_0$. Re_0 is a reference Reynolds defined as $\mathrm{Re}_0 \equiv \sqrt{15}\, C_\varepsilon^{-2/3}\, [P|^{\max}]^{1/6} \ell^{2/3} \nu^{-1/2}$ corresponding to Re_λ in a statistically steady-state. The factor of $(3/2)^{5/2}$ allows for a direct comparison with experimentally measured surrogates.

when the kinetic-energy loss-rate of the fine scales saturates at about half of the dissipation (see Fig. 2). This is non-trivial and implies that in equilibrium decaying turbulence the rate of kinetic energy loss for large ($k < k_c$) and small scales ($k \gtrsim k_c$) is roughly the same, i.e.,

$$\varepsilon = \int_0^\infty -\partial E(k,t)/\partial t\, dk = \overbrace{\int_0^{k_c} -\partial E(k,t)/\partial t\, dk}^{\approx \varepsilon/2} + \underbrace{\int_{k_c}^\infty -\partial E(k,t)/\partial t\, dk}_{\approx \varepsilon/2} \quad (4)$$

[note that $-\varepsilon = \int_0^\infty \partial E(k,t)/\partial t\, dk$ is a corollary of Eq. (1)]. Since, by virtue of Eq. (1), the large-scale kinetic energy loss rate is equal to the energy transferred to fine scales, the empirical relation (4) suggests that $\Pi = -\int_0^{k_c} \partial E(k,t)/\partial t\, dk \approx -\int_{k_c}^\infty \partial E(k,t)/\partial t\, dk \approx \varepsilon/2$, or simply $2\Pi \approx \varepsilon$ and thus $2C_\Pi \approx C_\varepsilon$. Interestingly, this may elucidate why C_ε assessed in statistically stationary turbulence up to $\mathrm{Re}_\lambda = \mathcal{O}(10^3)$ is typically $C_\varepsilon \approx 0.5$ [14,22] (consistent with our stationary data where $C_\varepsilon \approx C_\Pi \approx 0.5$, see Fig. 3) which is in stark contrast with freely decaying turbulence data where $C_\varepsilon \approx 1.0$–$1.4$ also up to $\mathrm{Re}_\lambda = \mathcal{O}(10^3)$ [13,14,21] (also consistent with our equilibrium decay data where $C_\varepsilon \approx 2C_\Pi \approx 1.2$, see Fig. 3).

Note that our findings do not invalidate the existence of a time-lag caused by the downscale energy transfer and, in fact, the change in the shape of the energy transfer spectrum throughout the transient may be a signature of that time-lag [see Figs. 4(a),(b)].

Finally we note in passing that the cascade flux/dissipation imbalance is also reflected in an imbalance between vortex stretching, $\omega_i\omega_j s_{ij}$ and enstrophy destruction, $2\nu\nabla\omega_i\nabla\omega_i$ (ω_i is the vorticity, s_{ij} the strain rate tensor and $\omega_i\omega_i$ is the enstrophy; we refer to quantities averaged over the whole computational domain). The imbalance $[\omega_i\omega_j s_{ij}/(2\nu\nabla\omega_i\nabla\omega_i) - 1]$ varies between -15% to $+25\%$ in the power input cycles and for the decay it grows throughout the non-equilibrium period until it saturates at about -25% when the equilibrium period is reached (not shown here).

The present findings highlight the importance of distinguishing Π and ε as two separate quantities which instantaneously can differ not only locally [23] but also globally, as our data show. It thus questions the use of ε as the scalar statistical quantity characterizing the inertial-range statistics in detriment of the actual energy cascade flux [23]. Our results together with the data available in the literature suggest that the imbalance between Π and ε occurs for a wide range of Reynolds numbers, at least up to $\mathrm{Re}_\lambda = \mathcal{O}(10^4)$. Whether the balance is recovered for even higher Reynolds number can only be asserted by massive computer simulations and high Reynolds number facilities. This strongly suggests that the constitutive relations $C_\varepsilon \approx$ constant and $\Pi = \varepsilon$, which are heavily used in state-of-the-art turbulence models, need to be replaced by the more robust empirical relations such as $C_\Pi \approx$ constant and a transport equation relating Π and ε analogous to Eq. (2). The related imbalance between vortex stretching and destruction also has direct implications in the modeling strategy of the dissipation equation.

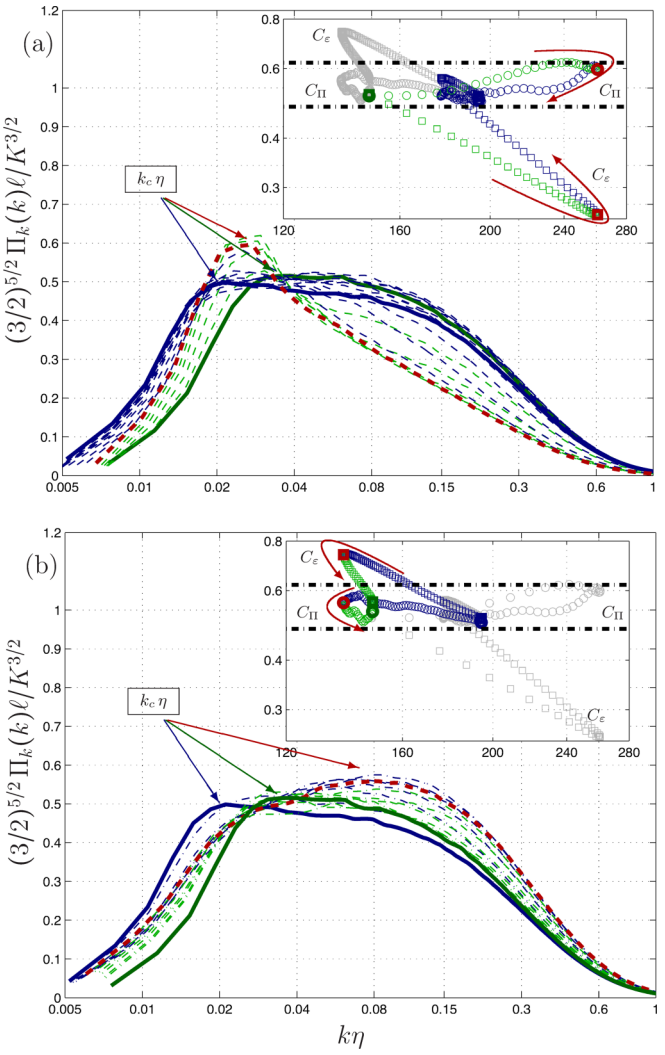

FIG. 4. (Color online) Throughout the power input cycle the energy transfer flux spectrum $\Pi_k(k) \equiv \int_0^k T(k',t)\,dk'$ is deformed even though the maximum normalized energy cascade flux $C_\Pi \equiv \max[\Pi_k(k)]\ell/K^{3/2}$ is roughly constant (see insets). Note that the Π_k deforms differently for transients caused by (a) a power input increase or (b) a power input decrease. The thick solid blue (dark gray) and green (light gray) lines, represent $\Pi_k(k)$ for quasi-stationary turbulence at the lower and higher power input states of the cycle (also marked with thick symbols in the insets). The dashed blue (dark gray) and green (light gray) lines represent the $\Pi_k(k)$ for a few snapshots while Re_λ is decreasing or increasing, respectively—see also inset where the arrows indicate the time evolution of C_ε and C_Π versus Re_λ throughout one square wave cycle.

ACKNOWLEDGMENTS

P.C.V. and C.B.S. acknowledge the support from Fundação para a Ciência e a Tecnologia (PTDC/EME-MFE/113589/2009). Some of the numerical simulations presented were carried out on the supercomputer system (NEC SX-9) in the Japan Agency for Marine-Earth Science and Technology. P.C.V. would like to thank the Japan Agency for Marine-Earth Science and Technology for their kind hospitality during his short stay at the Center for Earth Information Science and Technology and Dr. Luisa Pires for continuous feedback on the manuscript.

APPENDIX A: ZERO-CROSSING OF THE TRANSFER SPECTRUM AND THE INERTIAL-RANGE CONTRIBUTION TO DISSIPATION

In this appendix we summarize the evidence of a single zero-crossing of the transfer spectrum for any finite value of the viscosity. We also illustrate the non-negligible dissipation within the inertial-range for any Reynolds number, which motivate our definition of dissipative scales.

Following Ref. [24], for homogeneous stationary turbulence with a concentrated external forcing at low wave numbers, such as the present one, the low wave number transfer spectrum is approximately equal to the external forcing spectrum,

$$T(k) \approx -f(k) \quad \text{for} \quad 0 < k < k_F^{\max}, \tag{A1}$$

whereas for $k > k_F^{\max}$ the transfer spectrum $T(k)$ must change sign [since $\int_0^\infty T(k,t)\,dk = 0$] and by virtue of Eq. (1) take the form

$$T(k) = 2\nu k^2 E(k) \quad \text{for} \quad k > k_F^{\max}, \tag{A2}$$

since $f(k > k_F^{\max}) = 0$ and $\partial E/\partial t = 0$. A Kolmogorov-Obukhov inertial-range spectrum $E(k) = C_K \varepsilon^{2/3} k^{-5/3}$ thus leads to a transfer spectrum following $T(k) = C_K \nu\, \varepsilon^{2/3} k^{1/3}$ which implies that, at finite ν, there is no actual range of scales where $T(k) = 0$ [9,19,25]. Nevertheless, it will visually appear (and may be reasonably approximated for practical purposes) as a plateau [c.f. Fig. 5(b)], just like a parabola $y = c\,x^2$ will appear to have a plateau around $x = 0$ as the constant c becomes vanishingly small (see, e.g., Fig. 5 in Ref. [26] and Fig. 4 in Ref. [27]). Nevertheless, this illustrates that there is only a single wave number, which we denote as k_c, where the transfer spectrum is identically zero, i.e., $T(k_c) = 0$.

We confirm this in our data for statistically stationary period within dataset 2 (i.e., $\partial E/\partial t \approx 0$, see Table I) at $\mathrm{Re}_\lambda \approx 190$ [see Fig. 5(a)]. Notice that at these Reynolds numbers the turbulence is strong enough for the onset of a power-law region in the velocity spectrum which is reasonably fitted with the Kolmogorov-Obukhov prediction [4] of $E = C_K \varepsilon^{2/3} k^{-5/3}$ for the inertial-range scales, $4 \lessapprox k \lessapprox 32$. Note that we have averaged each of the terms for about two eddy turnover times $\ell/\sqrt{K}$.

We also illustrate this behavior at larger Reynolds numbers [see Fig. 5(b)] employing a model velocity spectrum, $E(k)$ [4],

$$E(k) = C_K\, \varepsilon^{2/3} k^{-5/3} \left(\frac{k\ell}{\sqrt{(k\ell)^2 + c_\ell}} \right)^{5/3+2} \times \exp\left(-\beta \left\{ \left[(k\eta)^4 + c_\eta^4 \right]^{1/4} - c_\eta \right\} \right) \tag{A3}$$

with the constants $C_K = 1.5, c_\ell = 6.78, c_\eta = 0.4, \beta = 5.2$ and we arbitrarily set $\varepsilon = \ell = 1$ and $\nu = 9 \times 10^{-7}$, so that $\mathrm{Re}_\lambda = 50\,000$. For stationary turbulence $[\partial E(k,t)/\partial t = 0]$ with a prescribed external forcing, this model spectrum completely determines the energy transfer spectrum $T(k,t)$ from Eq. (1). The external forcing spectrum we use in our DNSs is a discrete version of a Gaussian shaped function [16],

$$f(k) \sim \exp\left(\frac{(k - k_f)^2}{c} \right) \quad \text{for} \quad k \leqslant k_F^{\max}, \tag{A4}$$

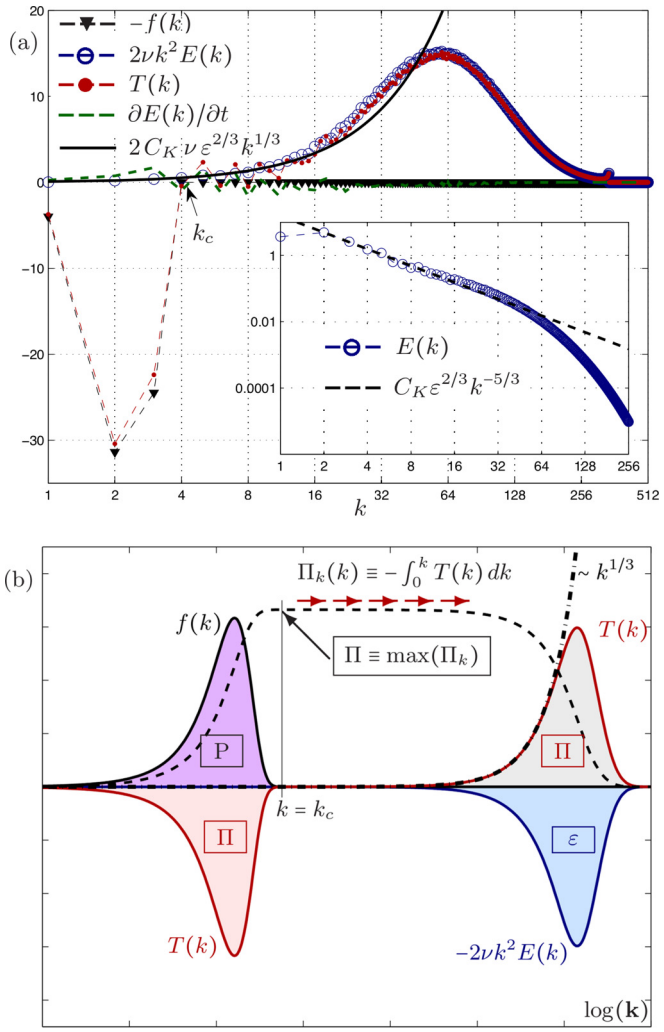

FIG. 5. (Color online) Terms of the power balance, Eq. (1), for (a) the $N = 1024^3$ simulation data in a statistically stationary period and (b) based on a model spectrum at $\mathrm{Re}_\lambda = 50\,000$. Since the data are plotted against the wave number in logarithmic coordinates all the curves have been pre-multiplied by k to keep the visual area in the plot proportional to the area of the integral. In the inset of (a) the velocity spectrum E is plotted together with the Kolmogorov-Obukhov inertial-range spectrum, $E(k) = C_K \varepsilon^{2/3} k^{-5/3}$ and the corresponding transfer spectrum, $T(k) = C_K\, \nu\, \varepsilon^{2/3} k^{1/3}$, is added to the main plot. The numerical value used for the Kolmogorov constant is $C_K = 1.7$.

where k_f and c determine the wave number of $\max[f(k)]$ and the degree of concentration, respectively, and $k_F^{\max}$ is the maximum wave number with external power input.

Our data, as well as the model spectrum, illustrate the non-negligible contribution of the inertial range to the overall dissipation, even though their principal role is to transfer energy to smaller scales. An inertial-range Kolmogorov-Obukhov spectrum leads to a dissipation spectrum following $2\,C_K\,\nu\,\varepsilon^{2/3}k^{1/3}$ [Fig. 5(b)]. This also reasonably approximates our data for $2 \leqslant k \leqslant 32$ [Fig. 5(a)]. Note that for $16 \leqslant k \leqslant 32$ the spectrum becomes slightly shallower than $k^{-5/3}$ prior to the viscous roll-off, which is usually denoted as a pre-dissipative bump or bottleneck effect. It should be clear, therefore, that the region of the dissipation

spectrum which increases with the wave number corresponds mostly to the inertial-range and therefore it is always responsible for a non-negligible fraction of the dissipation, regardless of how large the Reynolds number is. Conversely, within the fine-scales the spectra rolls off exponentially (or at least significantly faster than k^{-2}) which corresponds to the remaining contribution (about half) of the dissipation.

APPENDIX B: LEADING ORDER RESPONSE OF TURBULENCE TO POWER INPUT CHANGES

To find the leading order response of statistically stationary turbulence to a change in the energy cascade flux we approximate $T(k,t)$, $E(k,t)$, and $f(k,t)$ by Taylor polynomials around t_0, corresponding to the instant where the forcing was switched off (i.e., for $t < t_0$ turbulence is statistically steady and for $t \geqslant t_0$ it is freely decaying), i.e.,

$$\begin{aligned} E(k,t) &= E^{(0)}(k,t_0) + E^{(1)}(k,t_0)\,t + \frac{1}{2}E^{(2)}(k,t_0)\,t^2 + \mathcal{O}(t^3), \\ T(k,t) &= T^{(0)}(k,t_0) + T^{(1)}(k,t_0)\,t + \mathcal{O}(t^2), \\ f(k,t) &= f^{(0)}(k,t_0) + f^{(1)}(k,t_0)\,t + \mathcal{O}(t^2), \end{aligned} \tag{B1}$$

where $E^{(n)}(k,t)$, $T^{(n)}(k,t)$, and $f^{(n)}(k,t)$ represent the nth partial derivatives with respect to time. We consider a large scale forcing $f^*(k)$ (time invariant prior to being switched off) that does not inject energy on dissipative scales (i.e., scales corresponding to $k \geqslant k_c$),

$$f(k,t) = \begin{cases} f^*(k) = \begin{cases} \neq 0 & 0 < k < k_c \\ 0 & \text{otherwise} \end{cases} & \text{for} \quad t < t_0 \\ 0 & \text{for} \quad t \geqslant t_0. \end{cases} \tag{B2}$$

Introducing Eq. (B1) in Eq. (1) and gathering the terms by their time dependence leads to

$$t^0 : \; E^{(1)}(k,t_0) = T^{(0)}(k,t_0) - 2\nu k^2 E^{(0)}(k,t_0) + f^{(0)}(k,t_0), \tag{B3}$$

$$t^1 : \; E^{(2)}(k,t_0) = T^{(1)}(k,t_0) - 2\nu k^2 E^{(1)}(k,t_0) + f^{(1)}(k,t_0). \tag{B4}$$

For $t < t_0$ the turbulence is stationary and $E^{(1)}(k,t) = 0$, but at $t = t_0$ the forcing is set to zero and the rate of loss of kinetic energy per wave number is initially the same as the power that was being supplied by the external forcing, i.e.,

$$E^{(1)}(k,t) = \begin{cases} \begin{cases} 0 & \text{if} \quad t < t_0 \\ f^*(k) & \text{if} \quad t = t_0 \end{cases} & \text{for} \quad k < k_c \\ 0 & \text{for} \quad k \geqslant k_c, t \leqslant t_0. \end{cases} \tag{B5}$$

This can be introduced in Eq. (B4) to get [noticing that $f^{(n)}(k > k_c,t) = 0$],

$$E^{(2)}(k,t_0) = T^{(1)}(k,t_0) \qquad \text{for} \quad k > k_c, \tag{B6}$$

which in turn can be inserted back into Eq. (B1) to conclude that, for $k > k_c$

$$\begin{aligned} E(k,t) &= E^{(0)}(k,t_0) + \tfrac{1}{2}T^{(1)}(k,t_0)\,t^2 + \mathcal{O}(t^3) \\ T(k,t) &= T^{(0)}(k,t_0) + T^{(1)}(k,t_0)\,t + \mathcal{O}(t^2). \end{aligned} \tag{B7}$$

Note that it is likely that $T^{(1)}(k,t_0) \neq 0$ since the loss of large scale kinetic energy K for $t \geqslant t_0$ [c.f. Eq. (B5) for $k < k_c$] will likely have an immediate effect on the the energy transferred to small scales, since as it is shown in the main paper that $\Pi = \int_0^{k_c} -T(k,t)\,dk \sim K^{3/2}/\ell$, and therefore we expect $\partial\Pi/\partial t|_{t\geqslant t_0} \neq 0$, which is supported by our data (see Figs. 2 and 3).

We can multiply $E(k,t)$ by $2\nu k^2$ to get the dissipation spectrum and integrate Eq. (B7) over the wave numbers $k_c \leqslant k < \infty$, i.e.,

$$\begin{aligned} \varepsilon' &\equiv \int_{k_c}^{\infty} 2\nu k^2 E(k,t)\,dk = \varepsilon'(t_0) + \frac{1}{2}\left.\frac{\partial\Pi}{\partial t}\right|_{t=t_0} t^2 + \mathcal{O}(t^3) \\ \Pi &\equiv \int_{k_c}^{\infty} T(k,t)\,dk = \Pi(t_0) + \left.\frac{\partial\Pi}{\partial t}\right|_{t=t_0} t + \mathcal{O}(t^2), \end{aligned} \tag{B8}$$

which, due to the fact that $\Pi(t_0) = \varepsilon'(t_0)$, leads to the desired result

$$\Pi(t) - \varepsilon'(t) = \left.\frac{\partial\Pi}{\partial t}\right|_{t=t_0} t + \mathcal{O}(t^2) \quad \text{for} \quad t \geqslant t_0. \tag{B9}$$

[1] G. Falkovich, A. Fouxon, and M. Stepanov, Nature **419**, 151 (2002); V. Dallas and J. C. Vassilicos, Phys. Rev. E **84**, 046315 (2011).

[2] A. Johansen, J. S. Oishi, M.-M. Mac Low, H. Klahr, T. Henning, and A. Youdin, Nature **448**, 1022 (2007).

[3] A. Mafra-Neto and R. T. Cardé, Nature **369**, 142 (1994); M. Vergassola, E. Villermaux, and B. I. Shraiman, *ibid.* **445**, 406 (2007); D. R. Webster and M. J. Weissburg, Annu. Rev. Fluid Mech. **41**, 73 (2009).

[4] U. Frisch, *Turbulence: The Legacy of A. N. Kolmogorov* (Cambridge University Press, Cambridge, 1995); S. B. Pope, *Turbulent Flows* (Cambridge University Press, Cambridge, 2000).

[5] G. L. Eyink, Nonlinearity **16**, 137 (2003).

[6] C. Meneveau and J. Katz, Annu. Rev. Fluid Mech. **32**, 1 (2000).

[7] W. K. George, in *International Colloquium on Fundamental Problems of Turbulence, 50 Years after the Turbulence Colloquium Marseille 1961*, edited by M. Farge, H. K. Moffatt, and K. Schneider (EDP Sciences, Paris, 2014).

[8] R. Onishi and J. C. Vassilicos, J. Fluid Mech. **745**, 279 (2014).

[9] R. A. Antonia and P. Burattini, J. Fluid Mech. **550**, 175 (2006); J. Tchoufag, P. Sagaut, and C. Cambon, Phys. Fluids **24**, 015107 (2012).
[10] J. L. Lumley, Phys. Fluids A **4**, 203 (1992); A. Yoshizawa, Phys. Rev. E **49**, 4065 (1994); R. Rubinstein, T. T. Clark, D. Livescu, and L.-S. Luo, J. Turb. **5**, 1 (2004); W. J. T. Bos, L. Shao, and J.-P. Bertoglio, Phys. Fluids **19**, 045101 (2007); K. Horiuti and T. Tamaki, *ibid.* **25**, 125104 (2013).
[11] A. Kuczaj, B. Geurts, D. Lohse, and W. van de Water, Comput. Fluids **37**, 816 (2008).
[12] P. C. Valente and J. C. Vassilicos, Phys. Rev. Lett. **108**, 214503 (2012).
[13] P. C. Valente and J. C. Vassilicos, arXiv:1307.5901.
[14] P. Burattini, P. Lavoie, and R. A. Antonia, Phys. Fluids **17**, 098103 (2005).
[15] C. B. da Silva and J. C. F. Pereira, Phys. Fluids **20**, 055101 (2008).
[16] K. Alvelius, Phys. Fluids **11**, 1880 (1999).
[17] S. M. de Bruyn Kops and J. J. Riley, Phys. Fluids **10**, 2125 (1998).
[18] P. C. Valente and J. C. Vassilicos, Phys. Lett. A **376**, 510 (2012).
[19] W. D. McComb, J. Phys. A: Math. Theor. **41**, 075501 (2008).
[20] W. D. McComb, A. Berera, M. Salewski, and S. Yoffe, Phys. Fluids **22**, 061704 (2010).
[21] K. R. Sreenivasan, Phys. Fluids **27**, 1048 (1984).
[22] K. R. Sreenivasan, Phys. Fluids **10**, 528 (1998).
[23] R. Kraichnan, J. Fluid Mech. **62**, 305 (1974).
[24] T. Ishihara, T. Gotoh, and Y. Kaneda, Annu. Rev. Fluid Mech. **41**, 165 (2009).
[25] K. N. Helland and C. W. Van Atta, J. Fluid Mech. **79**, 337 (1977).
[26] T. Watanabe and T. Gotoh, J. Fluid Mech. **590**, 117 (2007).
[27] Y. Kaneda, T. Ishihara, M. Yokokawa, K. Itakura, and A. Uno, Phys. Fluids **15**, 21 (2003).